

# PROCEEDINGS OF SPIE

[SPIDigitalLibrary.org/conference-proceedings-of-spie](https://spiedigitallibrary.org/conference-proceedings-of-spie)

## The combination design for open and endoscopic surgery using fluorescence molecular imaging technology

Yamin Mao  
Shixin Jiang  
Jinzuo Ye  
Yu An  
Xin Yang  
Chongwei Chi  
Jie Tian

# The Combination Design for Open and Endoscopic Surgery Using Fluorescence Molecular Imaging Technology

Yamin Mao<sup>a</sup>, Shixin Jiang<sup>b</sup>, Jinzuo Ye<sup>a</sup>, Yu An<sup>b</sup>, Xin Yang<sup>a</sup>, Chongwei Chi<sup>\*a</sup>, Jie Tian<sup>\*a</sup>

<sup>a</sup>Key Laboratory of Molecular Imaging, Institute of Chinese Academy of Sciences, Beijing 100190, China; <sup>b</sup>The Department of Biomedical Engineering, School of Computer and Information Technology, Beijing Jiaotong University, Beijing 100044, China

## ABSTRACT

For clinical surgery, it is still a challenge to objectively determine tumor margins during surgery. With the development of medical imaging technology, fluorescence molecular imaging (FMI) method can provide real-time intraoperative tumor margin information. Furthermore, surgical navigation system based on FMI technology plays an important role for the aid of surgeons' precise tumor margin decision. However, detection depth is the most limitation exists in the FMI technique and the method convenient for either macro superficial detection or micro deep tissue detection is needed. In this study, we combined advantages of both open surgery and endoscopic imaging systems with FMI technology. Indocyanine green (ICG) experiments were performed to confirm the feasibility of fluorescence detection in our system. Then, the ICG signal was photographed in the detection area with our system. When the system connected with endoscope lens, the minimum quantity of ICG detected by our system was 0.195 ug. For aspect of C mount lens, the sensitivity of ICG detection with our system was 0.195ug. Our experiments results proved that it was feasible to detect fluorescence images with this combination method. Our system shows great potential in the clinical applications of precise dissection of various tumors.

**Keywords:** Intraoperative image-guided surgery, fluorescence molecular imaging, surgical navigation system, indocyanine green, endoscopy

## 1. INTRODUCTION

Cancer curing rate is largely dependent on the removing extent of residual cancer tissues, which is still relay on surgeons' skills and experiences. Palpation and visual inspection usually used by surgeons are not enough to distinguish malignancy from norm tissue [1]. Therefore, developing fluorescence-guided surgery (FGS) to provide surgeons with more accurate tissue information would be an effective way to improve the precision of tumor resection. FGS refers to the use of an optical imaging method to provide surgeons with real-time fluorescent information of tumor margins in surgical oncology, which has the potential to dramatically change the operation in cancer surgeries [2].

Imaging system is introduced to FGS for reasons of that the naked eyes is invisible to fluorescence [3]. In terms of application, the imaging system generally fall into two categories: open-surgery imaging system (OIS) and endoscopic imaging system (EIS). OIS with a wide angle lens used for open surgeries, such as sentinel node mapping [4, 5], various tumor resection [6-8] and important structures (arteries and neuro) imaging [9]. EIS with an endoscopic lens used for minimally invasive surgeries, such as colorectal cancer[10], gastrointestinal surgery[11] and esophagus cancer [12]. However, limitation of detection depth exists in OIS and absence of wide view exists in the EIS. In clinical applications, we need a system to help surgeons to convenient switch from macro superficial detection to micro deep tissue detection.

In this work, we developed a novel imaging system named open-surgery and endoscopic imaging system (OEIS), which combines the advantages of OIS and EIS. To satisfy different imaging demand, we employed two lenses including a C mount lens for macro superficial detection and an endoscopic lens for micro deep tissue detection. Based on the fact of almost the entire endoscopic lens having a uniform industrial C interface, we also selected a wide angle C mount lens. NIR

---

\*chongwei.chi@ia.ac.cn; \*tian@iee.org, jie.tian@ia.ac.cn; Telephone: 8610-82618465; fax: 8610-62527995; Website:

<http://www.mitk.net> <http://www.3dmed.net>

light and white light collected from the camera lenses are divided into two beams by DC2 (DC2, Photometric, USA) and collected by the near-infrared (NIR) camera and the color camera, respectively. We also developed a software system for data storing and image processing. Finally, we performed a series of indocyanine green (ICG) experiments to demonstrate the sensitivity of our system and a Multi-Function Calibration Target (NT58-403, Edmund Optics, USA) to examine the system features. Our results shows that OEIS is suitable for various imaging-guided surgery applications.

## 2. METHODS AND MATERIALS

### 2.1 System Design

OEIS was developed by the Key Laboratory of Molecular Imaging of Chinese Academy of Sciences based on our previous studies[13, 14]. OEIS is made up of six parts: camera module (CM), system transformation module (STM), open-surgery imaging module (OIM), endoscopic imaging module (EIM), system supporting module (SSM) and data processing module (DPM), as shown in Figure. 1.

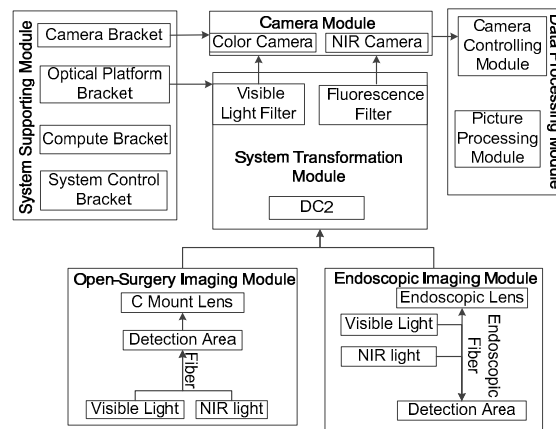


Figure 1. The hardware of OEIS.

CM. CM consists of two charge coupled device cameras (CCD), one is NIR camera (ProEM 1024B Excelon EMCCD, Princeton Instrument, USA) used to collect near infrared (NIR) fluorescence images, the other is color camera ( MVC 1300F-M00, Microview, China ) used to collect white-light images.

STM. STM includes a fluorescence filter (wavelength 810-870nm), a dual-channel imaging connection part (DC2, Photometrics, USA). With the help of this part, we can convenient change the imaging method from OIM to EIM.

OIM. A C mount lens (10456 Xenon 0.95-17, Schneider, Germany), a laser (MW-SGX-785, Changchun Lei Shi Optoelectronic Technology Co., Ltd., China) and a halogen lamp (KL2500LCD, SCHOTT, Germany) compose this module. The function of OIM is collecting light from a wide field of view and sending light to STM module.

EIM. We employed a rigid endoscope (WA53000A, OLYMPUS, Japan) for micro deep tissue detection. The endoscope has a 0 deg direction of view, a 70 deg visual field, 10 mm diameter and 300 mm length. A laser (MW-SGX-785, Changchun Lei Shi Optoelectronic Technology Co., Ltd., China) and a halogen lamp (KL2500LCD, SCHOTT, Germany) offers light for EIM. The function of this module is to detect deep tissue and send light to STM module.

SSM. SSM connects and supports every module of OEIS.

DPM. DPM is composed of camera controlling module(CCM) and picture processing module(PPM). CCM is used to adjust camera parameters and PPM is used to store, fuse and display images in real time.

#### 2.1.1 Endoscopic imaging design

The schematic of EIM as shown in Figure 2. The endoscope fiber moving in the deep detection area and collecting light from deep tissue. The white light and exciting light, meanwhile, through the endoscopic fiber to illuminate the detection area. Then the collected light is split into two parts by DC2 and collected by CM.

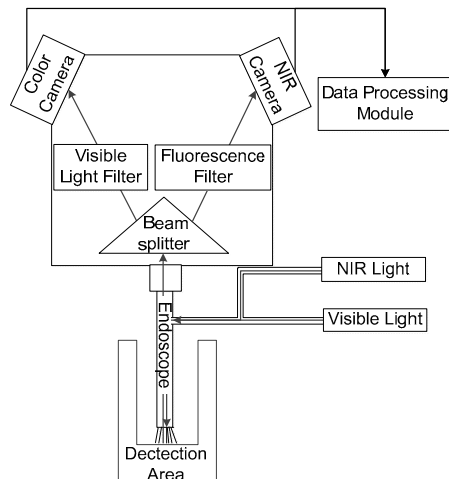


Figure 2. The schematic of endoscopic imaging module.

### 2.1.2 Open-surgery imaging design

The schematic of OIM was shown in Figure 3. We employed a wide-field lens connecting with STM to detect macro area. Furthermore, the white light and NIR light as light sources illuminate directly the detection area. Other parts of OIM schematic is the same as the EIM schematic.

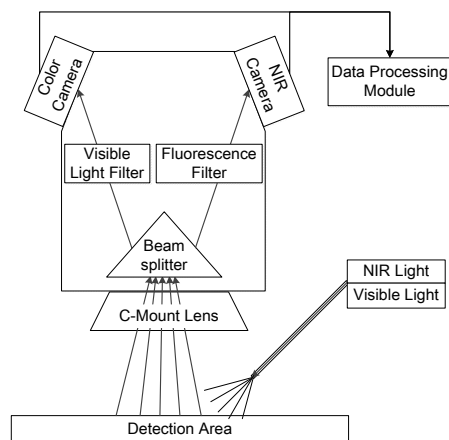


Figure 3. The schematic of open-surgery imaging module.

### 2.1.3 Dual-channel imaging design

The light collected from lens was transmitted through DC2 and split into two parts. Then NIR camera and color camera acquired images of the same region by connecting with the DC2. For the optical path designing, a fluorescence filter (wavelength 810-870nm) was placed in DC2 in front of the camera.

## 2.2 System Characterization

### 2.2.1 Optical characterization

The optical resolution of OEIS is tested with a Multi-Function Calibration Target. It allows the user to determine the maximal resolution of our system by finding the point at which the system loses contrast between adjacent lines. Test board calibration specifications included 5lp/mm, 10lp/mm, 20lp/mm, 30lp/mm, and 40lp/mm. The target allows testing the resolution of the system and the procedures are as follows.

1. Position the target in front of the cameras.

2. Properly focus the system and adjust the lighting to give the best contrast. If the lines are not visible, the spatial frequency is beyond that of the Lens and Camera combination. Use a smaller field of view with a higher magnification Lens.
3. Capture the image and import the image into an image analysis program in MATLAB.
4. Plot the intensity profile along a straight line perpendicular to the direction of the pattern lines.

### 2.2.2 Sensitivity measurements

ICG was purchased from Yichuang Pharmaceutical Limited Liability Company (Dandong, China) and stored at 4°C. The 4mg ICG powder is dissolved in 1ml of phosphate buffer synonymous (PBS) solution. 200 µl ICG solutions are added to the 96-well plate with a pipette. The serial ICG samples are prepared by 2 times the concentration gradient dilution with PBS ranging from 4mg/ml to  $1.22 \times 10^{-4}$  mg/ml with a volume of 200 µl. Then, the ICG signal is photographed in the detection area with our system.

## 2.3 System software Design

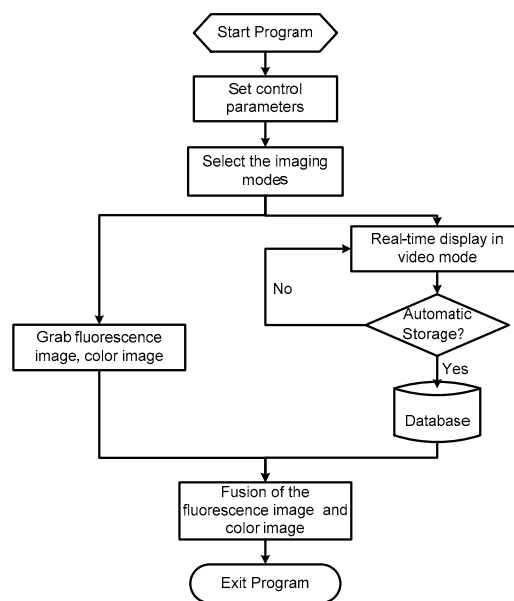


Figure 4. The design of system software framework.

The software user interface is designed based on QT3.2 and the image processing program is developed based on OpenCV1.0 and Visual C++ 6.0. Some algorithms are designed to help to achieve the performance of the software, for example, the correlation matching algorithm based on the average of the squared deviations.

In the part of control software, the parameters related to hardware structure and common settings are designed to control the cameras. The specific control parameters are shown below:

- ☐ Exposure time setting
- ☐ Shutter setting
- ☐ Electron multiplication (EM) gain mode
- ☐ Color mode/ gray-scale mode of the color camera
- ☐ Flip the images horizontally/vertically
- ☐ 90 degree rotation clockwise/counter clockwise of the images
- ☐ Timing of the automatic storage of video data

In order to facilitate surgeons operation during surgery, these parameters have been set to default after several tests, such as exposure time set to 0.02s, automatic storage interval set to 30s and fluorescence gray value range set to 0-500 et al.

### 3. RESULTS

#### 3.1 optical resolution test

The results to find the highest spatial frequency at which two lines can be distinguished from each other are shown in Figure 5. Figures 5. a and b are the images taken by color camera and NIR camera respectively with OIM. Figures 5. c and d are the analysis results of Figures 5. a and b. The horizontal axis represents the pixel number and the vertical axis represents the mean gray value of each pixel. Using the same method, we acquire figures 5. e, f, g and h with EIM. The results show that the maximum system optical resolution is 0.1mm (10lp/mm) both with the C mount lens and endoscope.

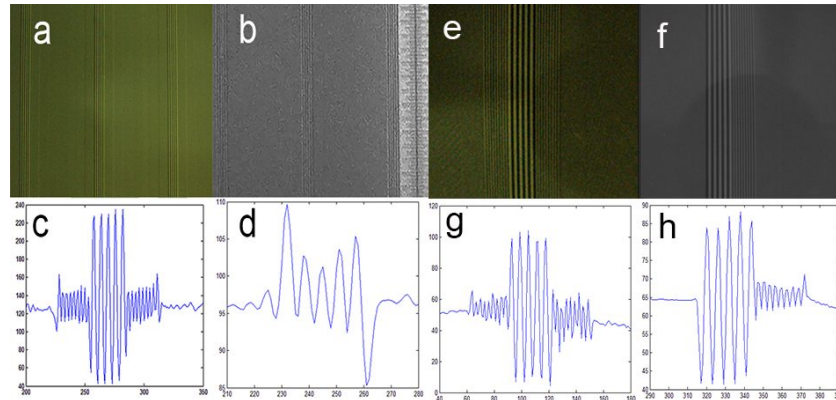


Figure 5. Spatial frequency of color camera and NIR camera. a. the picture taken by color camera with the C mount lens; b. the picture taken by NIR camera with the C mount lens; c. the analysis results of a; d. the analysis results of b; e. the picture taken by color camera with the endoscope; f. the picture taken by NIR camera with the endoscope; g. the analysis results of e; h. the analysis results of f.

#### 3.2 ICG fluorescence sensitivity test

The light intensity of each concentration is detected by our system shown in Figures. 6 and 7. Series dilution of ICG could be quantified after NIR light excitation. Figures. 6. a and b are obtained by NIR camera and color camera respectively with OIM. Figure. 6. c is the result processed through the image processing algorithms. Figure. 6. d is the quantization values of ICG solution in each hole. Since the concentration of the maximum intensity is  $7.81 \times 10^{-3}$  mg/ml, the minimum concentration is  $9.77 \times 10^{-4}$  mg/ml. Using the same method, we acquire figure. 7a, b, c and d with EIM. The concentration of the maximum intensity is  $7.81 \times 10^{-3}$  mg/ml, and the minimum detection concentration is  $9.77 \times 10^{-4}$  mg/ml. As a reason of the fluorescent quenching, high concentration solution of ICG is not bright.

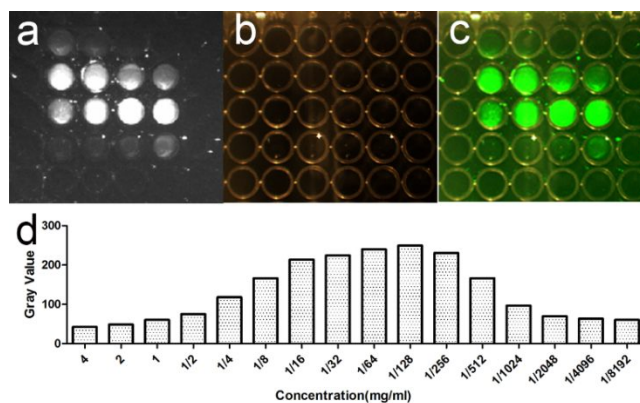


Figure 6. a The fluorescent image of ICG taken by color camera with OIM; b the color image of ICG taken by NIR camera with OIM; c merged image with a and b; d the quantization values of ICG solution in each hole.

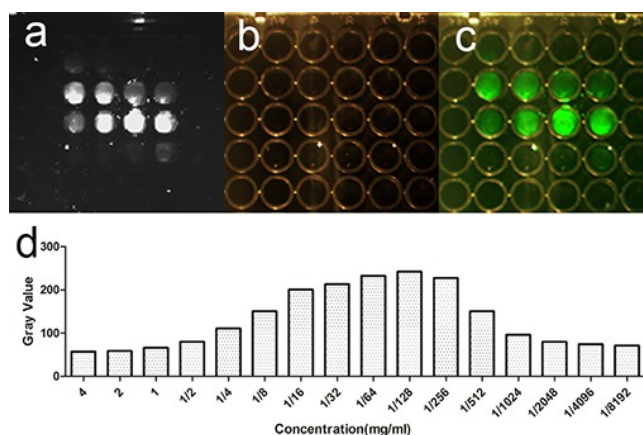


Figure 7. a The fluorescent image of ICG taken by color camera with EIM; b the color image of ICG taken by NIR camera with EIM; c merged image with a and b ; d the quantization values of ICG solution in each hole.

#### 4. DISCUSSION

Surgical navigation system combining with optical molecular imaging method as an auxiliary tool that can provide surgeons with tumor tissue information. With the development of surgical navigation systems, there are various types of systems used for open-surgeries [4-6] or minimally invasive surgeries [15, 16]. However, limitation of detection depth exists in the open-surgery intraoperative systems and absence of detection width exists in the endoscopic intraoperative systems. Our system combine the advantages of these two surgical navigation systems for providing surgeons with flexible switching from a wide field of view to a deep field of vision. A series of ICG experiments have proved that this system can collect fluorescence light either with a C mount lens or with an endoscopic lens. We chose ICG because ICG are already in clinical use. We hope OEIS can complete the clinical translation and be used in various surgical oncology in the near future.

#### 5. CONCLUSIONS

In summary, we designed OEIS that can flexibly switch the imaging field of view by combining advantages of both open-surgery and endoscopic imaging systems. The ICG experiment and multi-function calibration target test have proved the feasibility and performance of this system with either a C mount lens or an endoscopic lens. Future work will be focused on validating the feasibility of OEIS in preclinical studies and the clinical translation of OEIS and raise cure rate of tumor patients.

#### 6. ACKNOWLEDGEMENTS

This study was supported by the National Basic Research Program of China (973 Program) under Grant No. 2011CB707700, the National Natural Science Foundation of China under Grant No. 81227901, 61231004 , the National Key Technology R&D Program of China under Grant No. 2012BAI23B01, the Instrument Developing Project of the Chinese Academy of Sciences under Grant No. YZ201359, and National Natural Science Foundation of China No. 81470083.

#### REFERENCES

- [1] Vahrmeijer, A. L., Hutteman, M., Vorst, J. R. v. d., Velde, C. J. H. v. d., and Frangioni, J. V., "Image-guided cancer surgery using near-infrared fluorescence," *Nat Rev Clin Oncol. Papers* 10(9), 507-18 (2013).
- [2] Nguyen, Q. T., and Tsien, R. Y., "Fluorescence-guided surgery with live molecular navigation--a new cutting edge," *Nat Rev Cancer. Papers* 13(9), 653-62 (2013).
- [3] Keereweer, S., Kerrebijn, J. D., van Driel, P. B., Xie, B., Kaijzel, E. L., Snoeks, T. J., Que, I., Hutteman, M., van der Vorst, J. R., Mieog, J. S., Vahrmeijer, A. L., van de Velde, C. J., Baatenburg de Jong, R. J., and Lowik, C. W., "Optical image-guided surgery--where do we stand?," *Mol Imaging Biol. Papers* 13(2), 199-207 (2011).

- [4] Chi, C., Ye, J., Ding, H., He, D., Huang, W., Zhang, G., and Tian, J., "Use of Indocyanine Green for Detecting the Sentinel Lymph Node in Breast Cancer Patients: From Preclinical Evaluation to Clinical Validation," *Plos One. Papers* 8(12), e83927 (2013).
- [5] Ashitate, Y., Hyun, H., Kim, S. H., Lee, J. H., Henary, M., V. Frangioni, J., and Choi, H. S., "Simultaneous mapping of pan and sentinel lymph nodes for real-time image-guided surgery," *Theranostics. Papers* 4(7), 693-700 (2014).
- [6] Lee, B. T., Hutteman, M., Gioux, S., Stockdale, A., Samuel J. Lin, Ngo, L. H., and Frangioni, J. V., "The FLARE intraoperative near-infrared fluorescence imaging system: a first-in-human clinical trial in perforator flap breast reconstruction," *Plast Reconstr Surg. Papers* 126(5), 1472-81 (2010).
- [7] Verbeek, F. P. R., Vorst, J. R. v. d., Schaafsma, B. E., Hutteman, M., Bonsing, B. A., Leeuwen, F. W. B. v., Frangioni, J. V., Velde, C. J. H. v. d., Swijnenburg, R.-J., and Vahrmeijer, A. L., "Image-guided hepatopancreatobiliary surgery using near-infrared fluorescent light," *J Hepatobiliary Pancreat Sci. Papers* 19(6), 626-37 (2012).
- [8] Vorst, J. R. v. d., Hutteman, M., Mieog, J. S. D., Rooij, K. E. d., Kaijzel, E. L., and Vahrmeijer, A. L., "Near-infrared fluorescence imaging of liver metastases in rats using indocyanine green," *J Surg Res. Papers* 174(2), 266-71 (2012).
- [9] Ashitate, Y., Stockdale, A., Choi, H. S., Laurence, R. G., and Frangioni, J. V., "Real-time simultaneous near-infrared fluorescence imaging of bile duct and arterial anatomy," *J Surg Res. Papers* 176(1), 7-13 (2012).
- [10] Glatz, J., Varga, J., Garcia-Allende, P. B., Koch, M., Greten, F. R., and Ntziachristos, V., "Concurrent video-rate color and near-infrared fluorescence laparoscopy," *J Biomed Opt. Papers* 18(10), 101302 (2013).
- [11] Jenssen, C., Alvarez-Sanchez, M. V., Napoleon, B., and Faiss, S., "Diagnostic endoscopic ultrasonography: Assessment of safety and prevention of complications," *World Journal of Gastroenterology. Papers* 18(34), 4659-4676 (2012).
- [12] Ben-David, K., Sarosi, G. A., Cendan, J. C., Howard, D., Rossidis, G., and Hochwald, S. N., "Decreasing morbidity and mortality in 100 consecutive minimally invasive esophagectomies," *Surg Endosc. Papers* 26(1), 162-7 (2012).
- [13] Ye, J., Chi, C., Zhang, S., Ma, X., and Tian, J., "A near-infrared fluorescence-based surgical navigation system imaging software for sentinel lymph node detection," *Papers* 8935, 89351U (2014).
- [14] Chi, C., Du, Y., Ye, J., Kou, D., Qiu, J., Wang, J., Tian, J., and Chen, X., "Intraoperative Imaging-Guided Cancer Surgery: From Current Fluorescence Molecular Imaging Methods to Future Multi-Modality Imaging Technology," *Theranostics. Papers* 4(11), 1072-1084 (2014).
- [15] Matsui, A., Tanaka, E., Choi, H. S., Kianzad, V., Gioux, S., Lomnes, S. J., and Frangioni, J. V., "Real-time, near-infrared, fluorescence-guided identification of the ureters using methylene blue," *Surgery. Papers* 148(1), 78-86 (2010).
- [16] Oh, G., Yoo, S. W., Jung, Y., Ryu, Y. M., Park, Y., Kim, S. Y., Kim, K. H., Kim, S., Myung, S. J., and Chung, E., "Intravital imaging of mouse colonic adenoma using MMP-based molecular probes with multi-channel fluorescence endoscopy," *Biomed Opt Express. Papers* 5(5), 1677-89 (2014).